Scripta Materialia 157 (2018) 15–18

Contents lists available at ScienceDirect

Scripta Materialia

journal homepage: www.elsevier.com/locate/scriptamat

Regular Article

Influence of La substitution on local structural and photoluminescence properties of $SrTiO_3$:Pr phosphor

Lucas Angelini Deltreggia [a], Maria Inês Basso Bernardi [b], Alexandre Mesquita [a,*]

[a] Institute of Geosciences and Exact Sciences, São Paulo State University (Unesp), Rio Claro, SP, Brazil
[b] São Carlos Institute of Physics, University of São Paulo, USP, São Carlos, SP, Brazil

ARTICLE INFO

Article history:
Received 15 June 2018
Received in revised form 10 July 2018
Accepted 15 July 2018
Available online 27 July 2018

ABSTRACT

Pr^{3+}-doped perovskite-based $SrTiO_3$ phosphors have been developed as a potential red phosphor. In this paper, we report the substitution of La^{3+} ions for Sr^{2+} ions in order to promote Sr vacancies to further enhance photoluminescence. Given that the La content increases, an enhancement in the intensity of all emissions is observed, mainly for $^1D_2$–$^3H_4$ and $^3P_0$–$^3H_6$ transitions. This enhancement of photoluminescence emissions is associated with disorder in the lattice caused by La incorporation. Raman measurements and X-ray absorption near edge structure (XANES) spectra at the Ti K-edge identify this disorder as a function of the La content.

Luminescent materials, or phosphors, typically consist of a host material and an activator and are widely used in optoelectronic devices, such as lasers, solar concentrators, vacuum fluorescent displays, medical radiology equipment (including scintillators), field emission displays and light-emitting diodes [1–3]. Host materials for phosphors include sulfides, metaloxides, oxy-halides and perovskites [2, 4–6]. Concerning activators, remarkable progress has been observed in the development of rare earth ions as luminescent centers in different semiconductors due to their narrow emission bands (*f–f* interactions) and high internal quantum efficiencies. Promising applications exist in the field of photonics as solid state lasers and optoelectronic devices [6]. Among luminescent materials with rare earth ion activators, Pr^{3+}-doped inorganic materials are well known for their promising emission properties, in particular as red phosphors [1]. The three red emission lines arise from different origins of the $4f^2$–$4f^2$ transitions, i.e. $^1D_2$–$^3H_4$ (603 nm), $^3P_0$–$^3H_6$ (617 nm) and $^3P_0$–$^3F_2$ (650 nm), and occur in addition to two green emission lines ($^3P_1$–$^3H_5$ (530 nm) and $^3P_0$–$^3H_5$ (547 nm))and one blue-green emission line ($^3P_0$–$^3H_4$ (491 nm)) [1, 7].

Pr^{3+}-doped perovskite-based $SrTiO_3$ ($SrTiO_3$:Pr) phosphors have been developed as potential red phosphors for devices operating with low-energy electron excitation and present better physical and chemical stability compared to conventional sulfide compounds [8]. Nevertheless, $SrTiO_3$:Pr phosphors emit weak luminescence since the Pr^{3+} ions, which act as activators and emit the red luminescence, cannot directly absorb the radiation used for excitation [8]. However, the introduction of metal cations of different valences into the $SrTiO_3$ matrix can enhance the emission via a number of mechanisms. For example, lattice defects created by Al^{3+} incorporation can absorb the excitation radiation, acting as sensitizers, and transfer it to the Pr^{3+} ions, resulting in their characteristic red emission [8].Moreover, the doping of $SrTiO_3$:Pr^{3+} powders with divalent metal ions (Mg^{2+} and Zn^{2+}) forms impurity energy levels near the bottom of the conduction band that provide more efficient energy transfer from the matrix to the Pr^{3+} ions [8, 9]. Furthermore, replacement of Sr with a pair of Li^+ and Na^+ ions is believed to facilitate the formation of hole traps, increasing the probability of recombination of electrons with captured holes, thus raising the luminescence intensity [9]. Enhancement of luminescence is also observed as a result of the introduction of trivalent metal ions, such as Al^{3+}, Ga^{3+} and In^{3+}, substituting for Ti^{4+}, explained by the compensation for the Pr^{3+} charge in the site of Sr^{2+} ions and the higher degree of crystallinity [8, 9].

Substitutions of monovalent cations for Sr^{2+} and trivalent cations for Ti^{4+} are used in order to achieve charge compensation. A strontium vacancy can, however, be promoted to achieve charge compensation as Pr^{3+} is typically thought to occupy a Sr^{2+} site. In this case, the formula $Sr_{1-3x/2}Pr_xTiO_3$can be adopted and charge compensation occurs by $x/2$ formula units of Sr vacancies per formula unit of Pr^{3+}. Hence, in this paper we report the substitution of Sr^{2+} ions by trivalent La ions in order to promote more Sr vacancies than $x/2$ to compensate the additional positive charge. In principle, the disordered structure caused by Sr vacancies can originate from the lower symmetry at Pr^{3+} sites, which can mix opposite parity into 4*f* configurational levels, subsequently increasing the $^1D_2$–$^3H_4$ transition probabilities of Pr^{3+} ions and further enhance the luminescence of Pr^{3+} [10].

In this study, $Sr_{1-3(x+y)/2}Pr_xLa_yTiO_3$ (SLPT) samples ($x = 0.01$, $y = 0.05$ (SLPT5) and 0.10 (SLPT10)) were prepared by the polymeric precursor method, which has proven to be an effective procedure for the preparation of $SrTiO_3$ (ST) powders [11]. Strontium carbonate $SrCO_3$ (99%, Aldrich), titanium isopropoxide [$Ti(OC_3H_7)_4$] (98%, Aldrich),

* Corresponding author.
E-mail address: mesquita@rc.unesp.b (A. Mesquita).

https://doi.org/10.1016/j.scriptamat.2018.07.018
1359-6462/

praseodymium oxide Pr_2O_3 (99.9% Alfa Aesar), lanthanum nitrate hexahydrate (99%, Aldrich), ethylene glycol, $C_2H_6O_2$ (99.5%, Synth) and citric acid $C_6H_8O_7$ (99.5%, Synth) were used as raw materials. Titanium citrate was formed by titanium isopropoxide dissolution in a citric acid aqueous solution with constant stirring. The citrate solution was stirred at 70 °C to obtain a clear homogeneous solution. Stoichiometric quantities of strontium carbonate, lanthanum nitrate hexahydrate and praseodymium nitrate (Pr_2O_3 was dissolved with HNO_3 to convert into $Pr(NO_3)_3$) were added to the Ti citrate solution. After cation homogenization in the solutions, $C_2H_6O_2$ was added to promote a polyesterification reaction. The citric acid/ethylene glycol mass ratio was fixed at 60/40. As the preparation involves polymeric network formation, the samples were heated at 400 °C for 3 h to eliminate the organic precursors. After pyrolysis, all samples were annealed at 700 °C for 2 h.

Fig. 1 exhibits X-ray diffraction (XRD) patterns of the SLPT powders. These room-temperature measurements were performed in a RigakuUltima 4 powder diffractometer with geometry θ-2θ, with a rotating anode X-ray source (Cu-Kα radiation, $\lambda = 1.542$ Å) and a scintillation detector. The data were collected with a 0.02° step size at 5 s per step. As can be seen in Fig. 1, all samples crystallized and were indexed as cubic perovskite structures with *Pm3m* space group [10]. A small peak can be observed at ~25.2° and is assigned to the secondary phase of $SrCO_3$ with *Pmcn* space group [10]. In the $SrTiO_3$ matrix, Pr^{3+} can substitute for Sr^{2+} because their ionic radii are almost identical. The ionic radii of Pr^{3+} in the twelve and six-coordinated state are 1.30 and 0.99 Å, respectively, whereas the ionic radius of Sr^{2+} in the twelve-coordinated state is 1.44 Å. Given that the ionic radius of Ti^{4+} in the six-coordinated state is 0.605 Å [12], and since the samples were prepared considering the stoichiometric $Sr_{1-3/2(x+y)}Pr_xLa_yTiO_3$ formula, Pr^{3+} ions preferentially occupy Sr instead of Ti sites because of the similar ionic radii.

The local structure of SLPT samples was characterized by X-ray absorption spectroscopy at Ti K-edge measurements. X-ray absorption near edge structure (XANES) spectra give information on the coordination symmetry and the valence of ions incorporated in a solid. The energy of the absorption edge shifts according to the valence of the absorbing ion, since the binding energy of bound electrons rises as the valence increases. Also, the shape of the absorption edge depends on the unfilled local density of states and the coordination symmetry of the absorbing element. X-ray absorption spectra (4966 eV) were collected at the LNLS (National Synchrotron Light Laboratory, Brazil) facility using the D04B-XAS1 beamline. The LNLS storage ring was operated at 1.36 GeV and 100–160 mA. XANES spectra were collected

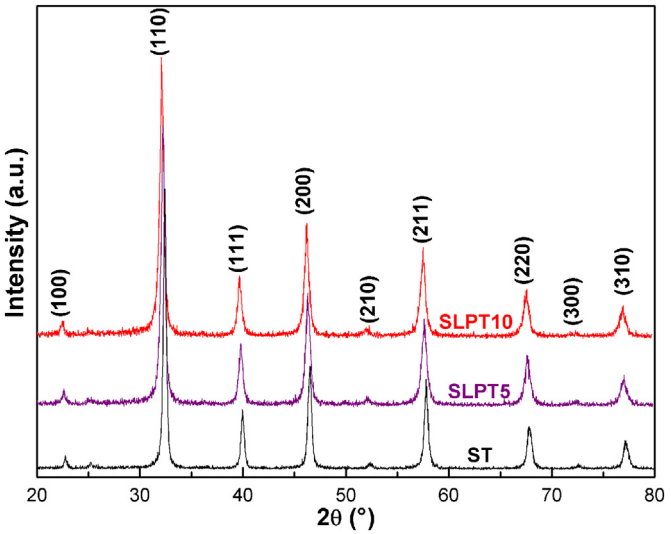

Fig. 1. X-ray diffraction for ST, SLPT5 and SLPT10 samples.

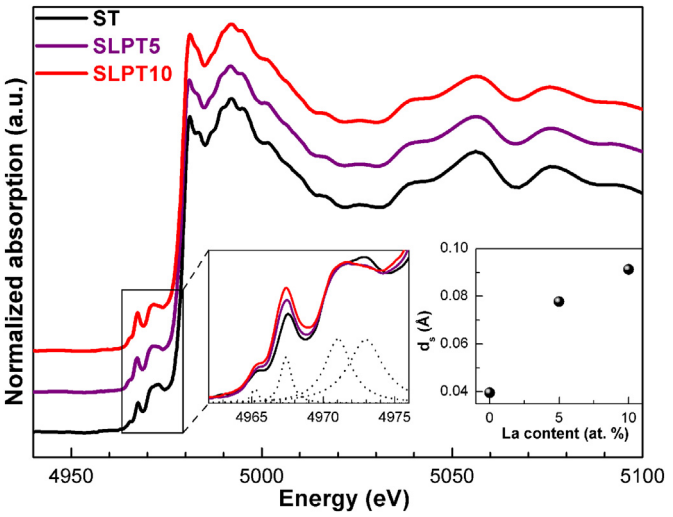

Fig. 2. XANES spectra at the Ti K-edge for ST, SLPT5 and SLPT10 samples. The lower-left inset magnifies the features in the pre-edge region. The lower-right inset shows the static off-center displacement (d_s) of Ti atoms in TiO_6 octahedra.

in transmission mode using a Si(111) channel-cut monochromator at room temperature. The spectra were analyzed through the Multi-Platform Applications for XAFS (MAX) software package [13].

Ti K-edge XANES spectra for SLPT samples are presented in Fig. 2. The lower-left inset of this figure shows in detail the four pre-edge transitions. The pre-edge region of the K-edge XANES spectra of some transition metal oxides is characterized by a pronounced feature occurring several volts before the main rising edge [14]. In transition metal oxides that crystallize in centrosymmetric structures, this pre-edge feature is small or absent, whereas in noncentrosymmetric structures, it can be quite large [14]. The peak at ~4966 eV has pure quadrupole origin due to the $1s(\mathrm{Ti}) \rightarrow 3d(t_{2g})(\mathrm{Ti})$ transition, whereas the peak at ~4967 eV is due to the $1s(\mathrm{Ti}) \rightarrow 4p(\mathrm{Ti})$ transition, including some degree of $1s(\mathrm{Ti}) \rightarrow 3d(e_g)(\mathrm{Ti})$ quadrupole contribution [10]. The overlapping peaks between 4969 and 4975 eV are assigned to a dipole excitation of 1*s* electrons to t_{2g} and e_g orbitals of the neighboring TiO_6 octahedra [10].

As can be seen in Fig. 2, the intensity of the peak at ~4967 eV increases as the amount of La increases. This increase has been associated with the fact that Ti ions must be present in the distorted octahedral environment and the area under this peak can be used to determine the off-center displacement in the TiO_6 octahedra of the $SrTiO_3$ perovskite structure [15, 16]. The static displacement (d_s) of Ti ions in the [001] direction was evaluated from the calculation of the area under this peak using a Lorentz function and an empirical relationship [15, 16]. The results are shown in the lower-right inset of Fig. 2, showing that the amount of La^{3+} increases with increasing the displacement of the Ti atom from the centrosymmetric position within the O octahedron. The small static off-center displacement observed is consistent with previous reports of 0.08 and 0.10 Å [16]. Nonetheless, this displacement indicates a small deviation from cubic symmetryand the La incorporation into the $SrTiO_3$ matrix implies local symmetry breaking. In principle, the Ti off-center displacement should be evaluated more precisely by an EXAFS (extended X-ray absorption fine structure) refinement of the octahedron TiO_6 first shell signal. However, the presence of the La L_{III}-edge 500 eV above the Ti K-edge limits drastically the EXAFS spatial resolution.

The Raman scattering technique is a useful tool to probe the disorder in the local crystal symmetry [17]. The $SrTiO_3$ cubic perovskite structure with space group *Pm3m* only presents the vibration modes $3F_{1u} + F_{2u}$ that are not Raman active, and no first-order Raman mode is expected in $SrTiO_3$ at room temperature [18]. Studies of the Raman spectra of $SrTiO_3$ have shown that the Raman modes can be modified, especially

the activation of the first-order modes, by many factors including strain effects, oxygen vacancies and even external conditions [17, 18]. Thus, each of the F_{1u} modes splits into a doubly degenerate E mode and a non-degenerate A_1 mode, while the F_{2u} mode splits into E and B_1 modes [18]. All of the A_1 and E modes are both Raman and infrared active, while the B_1 mode is Raman active. The presence of long-range electrostatic forces further splits each of the A_1 and E modes into transverse optical (TO) and longitudinal optical (LO) modes [18]. Therefore, the fundamental phonon modes of Slater-type (TO_1/LO_1), Last-type (TO_2/LO_2) and Axe-type (TO_4/LO_4), are probably present [17]. The lowest frequency TO_1/LO_1 modes arise due to B-ion motions against oxygen vibrations, the intermediate frequency TO_2/LO_2 modes originate from A-ion vibrations and the oxygen vibrations in BO_6 octahedra give rise to the highest frequency TO_4/LO_4 in the ABO_3 crystal lattice [17].

Fig. 3 shows the Raman spectra for SLPT samples. These spectra were measured at room temperature with a MonoVista CRS Raman spectrometer (S&I). The samples were irradiated with a laser beam focused by an Olympus microscope. For the excitation in backscattering geometry, the 633 nm line of a 35 mW He-Ne laser was used. The modes in the spectrum of the ST sample are assigned as follows: TO_1 (149 cm^{-1}), TO_2 (177 cm^{-1}), TO_3 (289 cm^{-1}), LO_2 (482 cm^{-1}), TO_4 (545 cm^{-1}), TO (730 cm^{-1}) and LO_4 (795 cm^{-1}). The peak observed at 1074 cm^{-1} is related to the $SrCO_3$ phase, in agreement with our XRD measurements [19]. Because the La^{3+} ions are incorporated in $SrTiO_3$ matrix, the intensity of TO_1, TO_3 and TO modes show a small increase, indicating that Ti sites are not affected by La addition. This result is in agreement with the XANES results, which show a small off-center displacement of Ti atoms as a function of La content. However, the intensity of TO_2 and LO_4 modes show a substantial increase with La content. Because the TO_2 mode originates from A-ion vibration in the ABO_3 structure, this increase is an indication of disorder at Sr sites due to La substitution and the formation of Sr vacancies. The behavior of the LO_4 mode denotes tilting of TiO_6 octahedra due to modified oxygen vibrations resulting from this disorder.

The photoluminescence spectra for SLTP5 and SLTP10 samples are show in Fig. 4. The spectra were measured at room temperature with a Thermal Jarrel-Ash Monospec monochromator and a Hamamatsu R446 photomultiplier. The 350.7 nm exciting wavelength of a krypton ion laser (Coherent Innova) was used; the output of the laser was maintained at 200 mW. The $^1D_2$–$^3H_4$, $^3P_0$–$^3H_6$, $^3P_0$–$^3F_2$, $^3P_1$–$^3H_5$, $^3P_0$–$^3H_5$ and $^3P_{0,1,2}$–$^3H_4$ transitions are indexed in the spectra of Fig. 4. As can be seen, the photoluminescence curve of the SLPT5 sample shows blue ($^3P_{0,1,2}$–$^3H_4$) and red ($^1D_2$–$^3H_4$ and $^3P_0$–$^3H_6$) emissions

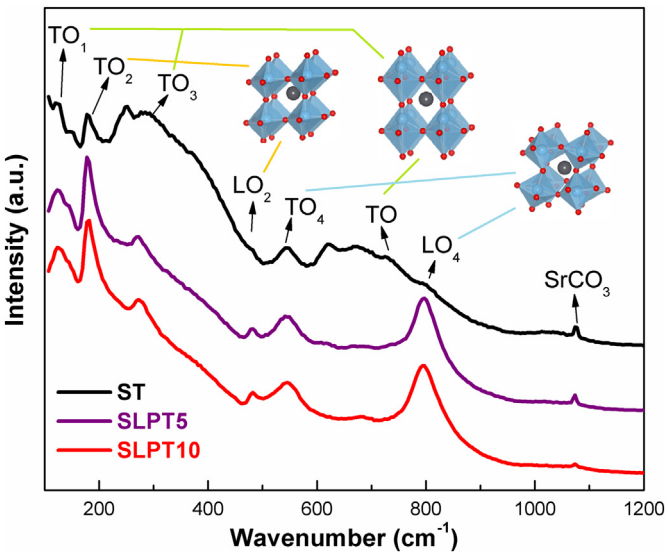

Fig. 3. Raman spectra for ST, SLPT5 and SLPT10 samples.

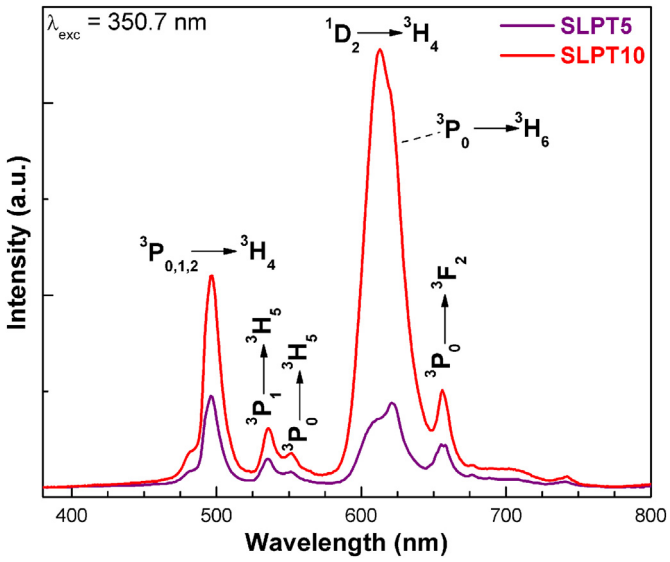

Fig. 4. Photoluminescence spectra for SLPT5 and SLPT10 samples.

with similar intensities. If the combination of the blue to red emissions can be regulated in a controlled manner, white emission from a single host may be realized, which can function as white light-emitting diodes (WLEDs) [1]. The spectrum of the SLPT10 sample shows an enhancement in the intensity of all emissions, mainly for $^1D_2$–$^3H_4$ and $^3P_0$–$^3H_6$ transitions.

It is well known that the photoluminescence efficiency of a rare earth ion is sensitive to the symmetry and strength of the crystal field and that an increased degree of distortion in the crystal field may enhance their luminescence efficiency [20]. According to Fujiwara et al. [20], in a study comparing $CaTiO_3$, $SrTiO_3$ and $BaTiO_3$ host lattices, Pr^{3+} substituted for the Ca^{2+} site in $CaTiO_3$:Pr can emit intense red light without the addition of enhancers, since $CaTiO_3$ has a distorted crystal structure due to the crystal framework constructed by tilted Ti octahedrons [20].Ions of large ionic radius or vacancies substituted for A-site ions tend to induce structural asymmetry in the host, approaching the lower symmetry around Pr^{3+} [10]. In principle, more uneven crystal fields due to the lower symmetry at the Pr^{3+} sites can mix opposite parity into 4*f* configurational levels, subsequently increasing the transition probabilities of Pr^{3+} ions [10].

Thus, we report the substitution of La^{3+} ions for Sr^{2+} ions in order to promote Sr vacancies to further enhance the photoluminescence of the $SrTiO_3$:Pr compound. Because the La content increases, all emission intensities are enhanced, mainly for $^1D_2$–$^3H_4$ and $^3P_0$–$^3H_6$ transitions. This enhancement of photoluminescence emissions is associated with disorder in the lattice caused by La incorporation. As shown by Raman and XANES measurements, disorder increases with tilting in the titanium octahedron cluster, the latter increasing with La content. Thus, the enhancement of the photoluminescence curves for $SrTiO_3$:Pr, La samples is associated with disorder in the $SrTiO_3$ lattice caused by La incorporation.

This work was supported by FAPESP (through project 2013/12993-4), CNPq (302743/2014-6) and LNLS (proposal number XAFS1-17750), Brazil. The authors also thank Leandro X. Moreno for Raman measurements.

References

[1] W. Tang, Y. Sun, M. Yu, X. Liu, Y.Q. Yin, B. Yang, L.M. Zheng, F. Qin, Z.G. Zhang, W.W. Cao, RSC Adv. 5 (35) (2015) 27491–27495.
[2] G.K. Ribeiro, F.S. Vicente, M.I.B. Bernardi, A. Mesquita, J. Alloys Compd. 688 (2016) 497–503.

[3] C.S. Lewis, H.Q. Liu, J.Y. Han, L. Wang, S.Y. Yue, N.A. Brennan, S.S. Wong, Nanoscale 8 (4) (2016) 2129–2142.
[4] J.L. Huang, L.Y. Zhou, Z.P. Liang, F.Z. Gong, J.P. Han, R.F. Wang, J. Rare Earths 28 (3) (2010) 356–360.
[5] A.A. Othman, M.A. Ali, E.M.M. Ibrahim, M.A. Osman, J. Alloys Compd. 683 (2016) 399–411.
[6] N.P. Bhagya, P.A. Prashanth, R.H. Krishna, B.M. Nagabhushana, R.S. Raveendra, Optik 145 (2017) 678–687.
[7] A. Brenier, I.V. Kityk, J. Appl. Phys. 90 (1) (2001) 232–236.
[8] H. Ryu, B.K. Singh, K.S. Bartwal, M.G. Brik, I.V. Kityk, AcMat 56 (3) (2008) 358–363.
[9] E.A. Bondarenko, A.A. Skomorokhov, N.I. Kargin, A.S. Gusev, S.M. Ryndya, OptSp 118 (5) (2015) 729–734.
[10] H.Q. Sun, Q.W. Zhang, X.S. Wang, Y. Zhang, Ceram. Int. 40 (10) (2014) 15669–15675.
[11] L.F. da Silva, J.C. M'Peko, J. Andres, A. Beltran, L. Gracia, M.I.B. Bernardi, A. Mesquita, E. Antonelli, M.L. Moreira, V.R. Mastelaro, J. Phys. Chem. C 118 (9) (2014) 4930–4940.
[12] R.D. Shannon, AcCrA 32 (SEP 1) (1976) 751–767.
[13] A. Michalowicz, J. Moscovici, D. Muller-Bouvet, K. Provost, J. Phys. Conf. Ser. 190 (2009), 012034.
[14] A. Mesquita, A. Michalowicz, V.R. Mastelaro, J. Appl. Phys. 111 (2012) 104110.
[15] H. Stocker, M. Zschornak, C. Richter, J. Hanzig, F. Hanzig, A. Hinze, K. Potzger, S. Gemming, D.C. Meyer, Scr. Mater. 86 (2014) 1–4.
[16] A.I. Frenkel, D. Ehre, V. Lyahovitskaya, L. Kanner, E. Wachtel, I. Lubomirsky, Phys. Rev. Lett. 99 (21) (2007).
[17] G. Jyothi, K.G. Gopchandran, Dyes Pigments 149 (2018) 531–542.
[18] X.E. Wu, D.J. Wu, X.J. Liu, Solid State Commun. 145 (5–6) (2008) 255–258.
[19] L.F. da Silva, W. Avansi, J. Andres, C. Ribeiro, M.L. Moreira, E. Longo, V.R. Mastelaro, Phys. Chem. Chem. Phys. 15 (29) (2013) 12386–12393.
[20] R. Fujiwara, H. Sano, M. Shimizu, M. Kuwabara, J. Lumin. 129 (2009) 231–237.